

Turing patterns with space varying diffusion coefficients: eigenfunctions satisfying the Legendre equation

Elkinn A. Calderón-Barreto, José L. Aragón*
Centro de Física Aplicada y Tecnología Avanzada,
Universidad Nacional Autónoma de México.
Boulevard Juriquilla 3001 Juriquilla 76230 Querétaro, Mexico.

November 28, 2022

Abstract

The problem of pattern formation in reaction-diffusion systems with space varying diffusion is studied. On this regard, it has already been shown that the necessary conditions for Turing instability are the same as for the case of homogeneous diffusion, but the sufficient conditions depend on the specific space dependence of the diffusion coefficient. In this work we consider the particular case when the operator of the spectral Sturm-Liouville problem associated with the general reaction-diffusion system has the Legendre polynomials as eigenfunctions. We then take a step forward, generalizing the standard weakly nonlinear analysis for these eigenfunctions, instead of the eigenfunctions of the Laplace operator. With the proposed generalization, conditions can be established for the formation of striped or spotted patterns, which are verified numerically, and compared with the case of homogeneous diffusion, using the Schnakenberg reaction diffusion system. Our results enrich the field of pattern formation and the generalization of the nonlinear analysis developed here can also be of interest in other fields as well as motivate further generalization by using general orthogonal functions.

*jaragon@unam.mx

1 Introduction

In a ground-breaking work from 1952 Alan Turing laid the foundations for chemical morphogenesis by proposing a reaction-diffusion theory for pattern formation [1]. Turing showed that two or more chemical substances, called morphogens, which react and diffuse in a medium such as a tissue, can induce stable periodic patterns through linear instability of a spatially uniform state. Turing's important discovery is that, under certain conditions, a stable spatially uniform state, in the absence of diffusion, can become unstable under nonuniform perturbations (introduced as random initial conditions) due to diffusion. This is the so-called Turing instability, which produces a spatially non-homogeneous steady state, that is, a spatial pattern. From a mathematical perspective, the Turing instability mechanism has two components. First, it is necessary to derive the necessary and sufficient conditions for diffusion-driven instability of the spatially uniform state and the initiation of the spatial pattern. This is achieved by a linear analysis, looking for a solution that grows in time; this analysis results in the selection of a dominant mode which is responsible for pattern initiation. Once the instability criterion is established, the determined dominant mode grows exponentially and is not valid at all times; and the long-time evolution of the pattern, and the determination of the type of pattern, should be studied by means of a nonlinear analysis [2].

The original Turing model became a master piece of mathematical modeling in biology and the best known model for explaining biological pattern formation. However, in recent years there have been great advances in understanding both the mathematical and biological aspects of this theory, including its generalization to a range of settings beyond the assumptions established by Turing [3, 4].

One possible generalization of the original theory is to consider spatial heterogeneity as a way to obtain irregular patterns. The experimental evidence that in some biological systems spatial inhomogeneities are important to regulate patterns lead to several generalizations of the reaction-diffusion problem: when one of the diffusion coefficients either depends on the spatial variables [5, 6] or is discontinuous [5, 7]; time-dependent [8] or concentration-dependent diffusion coefficients [9, 10, 11]; spatially varying parameters [12, 13]; reaction-diffusion system in a channel with the projected Fick-Jacobs-Zwanzig operator (with a diffusion coefficient that depends on the longitudinal coordinate) [14]; and pattern formation with superdiffusion

[15] or anomalous diffusion [16, 17]. A recent advance in the study of pattern formation in spatially heterogeneous reaction-diffusion systems was made in [18], where a more general instability criterion, which can be applied to spatially heterogeneous systems, was proposed as well as a procedure to calculate nonlinear mode coefficients as a way to understand the influences of each spatial mode on the long-time evolution of a pattern.

In this work, we consider the problem of a reaction-diffusion equation when the diffusion coefficient depends explicitly on the space variables, $\nabla \cdot (\mathcal{D}(\mathbf{x})\nabla \mathbf{u})$ for the particular case when the eigenfunctions of this operator are the Legendre polynomials, $L_p(x)$ in 1D and $L_{ij}(x, y) = L_i(x)L_j(x)$ in 2D. For this purpose, we used eigenfunction expansions, as in [19, 20, 18]. Using this approach, it has been shown that the linear stability properties of the system are the same as those of a reaction-diffusion system with constant diffusion coefficients [18]. The main contribution of this paper lies in the nonlinear analysis, where we propose a generalization of the standard weakly nonlinear analysis of the reaction-diffusion system using Legendre polynomials. The parameter regions for producing stripes or spots can be identified from the developed general nonlinear analysis.

Numerical simulations using finite elements were performed using the Schnakenberg system to verify the predictions of the proposed nonlinear analysis and to provide examples of one-dimensional and two-dimensional patterns, where the non-homogeneity of the final patterns, clearly influenced for the properties of the Legendre function, are visible.

The generalization of the standard nonlinear analysis using the orthogonal functions associated with the Legendre equations developed here can be of interest in the field of pattern formation and other areas such as climate modeling, where some one-dimensional models derived from the Budyko-Seller climate model contain a Legendre type operator as the studied in this work [21, 22].

2 Linear Turing analysis for spatially varying diffusion

Because the linear stability analysis is the first step in the mathematical study of pattern formation, in this section, we follow the generalization of the classical Turing instability analysis developed in [18] for various scenar-

ios of spatially heterogeneous systems, where spatially varying diffusion is a particular case. In this STUDY it is shown that the necessary conditions for Turing instability when the diffusion is homogeneous are the same as for the case of space varying diffusion coefficients, but the sufficient conditions may generally change. Henceforth, we will gather the results of this general theory applicable to our problem. This also allows us to establish essential ideas and notation.

The general non-dimensional form of a two-chemicals reaction-diffusion system with a space varying diffusion coefficient, is:

$$\frac{\partial \mathbf{u}}{\partial t} = D \nabla \cdot (\mathcal{D}(\mathbf{x}) \nabla \mathbf{u}) + \eta F(\mathbf{u}). \quad (1)$$

where $\mathbf{u} = (u, v)$ is a vector of two species defined on a bounded domain $\Omega \subset \mathbb{R}^n$, D is the diagonal matrix of diffusion coefficients D_u and D_v of u and v , respectively, $\mathcal{D}(\mathbf{x})$ is a function that describes the spatial variation of the diffusion rate, $F = (f, g)^T$ is the reaction kinetics, and η is a non-dimensional coefficient related to the size of the space domain. It is assumed that the system (1) is subject to Neumann (zero flux) boundary conditions:

$$\mathbf{n} \cdot (\mathcal{D}(\mathbf{x}) \nabla \mathbf{u}) = 0, \quad \text{on } \mathbf{x} \in \partial\Omega. \quad (2)$$

For simplicity, in what follows we assume $D_u = d$ and $D_v = 1$, that is, $D = \text{diag}[d, 1]$. This is equivalent to scaling (1) and does not imply a loss of generality.

By following the standard procedure, if $\mathbf{u} = \mathbf{u}_0 = (u_0, v_0)$ is a steady state, that is $\mathbf{f}(\mathbf{u}_0) = \mathbf{0}$, we consider a perturbation of the form $\mathbf{u}(\mathbf{x}, t) = \mathbf{u}_0 + \varepsilon \mathbf{v}(\mathbf{x}, t)$, where $0 < \varepsilon \ll 1$. The perturbation $\mathbf{v}(\mathbf{x}, t)$ is governed by the linear problem [18]:

$$\begin{aligned} \frac{\partial \mathbf{v}}{\partial t} &= D \nabla \cdot (\mathcal{D}(\mathbf{x}) \nabla \mathbf{v}) + \eta J \mathbf{v}, \quad \text{in } \Omega \\ \mathbf{n} \cdot (\mathcal{D}(\mathbf{x}) \nabla \mathbf{v}) &= 0, \quad \text{on } \partial\Omega, \end{aligned} \quad (3)$$

where J is the Jacobian matrix associated with the reaction kinetics F , evaluated at the steady state \mathbf{u}_0 .

Consider the spectral problem

$$\begin{aligned} \nabla \cdot (\mathcal{D}(\mathbf{x}) \nabla \Phi) &= -\rho \Phi, \quad \text{in } \Omega \\ \mathbf{n} \cdot (\mathcal{D}(\mathbf{x}) \nabla \Phi) &= 0, \quad \text{on } \partial\Omega. \end{aligned} \quad (4)$$

When solutions exist, there is an infinite but countable set of real eigenvalues ρ_i , which can be ordered according to increasing magnitude: $0 = \rho_0 < \rho_1 \leq \rho_2 \leq \dots$, and the corresponding set of eigenfunctions Φ_0, Φ_1, \dots , form a complete basis for functions on Ω satisfying the given boundary conditions. Therefore, it seems reasonable to propose a solution to (3) as a linear combination of eigenfunctions:

$$\mathbf{v}(\mathbf{x}, t) = \sum_{n=0}^{\infty} \mathbf{C}_n(t) \Phi_n(\mathbf{x}), \quad (5)$$

where $\mathbf{C}_n \in \mathbb{R}^2$, $n = 0, 1, 2, \dots$

Using all of the above, in [18] it is shown that the evolution of the k th Turing mode coefficient vector \mathbf{C}_k is given by

$$\frac{d\mathbf{C}_k}{dt} = (-\rho_m D + \eta J) \mathbf{C}_k, \quad k = 0, 1, 2, \dots, \quad (6)$$

which is the same system as that obtained for homogeneous diffusion, with the only difference being the eigenvalues ρ_m defined by the specific choice of $\mathcal{D}(\mathbf{x})$.

Assuming $\mathbf{C}_k(t) = e^{\lambda_k t} \mathbf{c}_k$, for \mathbf{c}_k a constant vector and $\lambda_k \in \mathbb{C}$, the values of λ_k for a Turing instability are given by the solution of the second order polynomial equation:

$$\lambda_k^2 - \alpha(\rho_k) \lambda_k + \beta(\rho_k) = 0, \quad (7)$$

where

$$\alpha(\rho_k) = \text{tr}(-\rho_k D + \eta J), \quad \text{and} \quad \beta(\rho_k) = \det(-\rho_k D + \eta J). \quad (8)$$

Linear stability is guaranteed if $\text{tr}(J) < 0$ and $\det(J) > 0$. For the steady state to be unstable to spatial perturbations we require $\text{Re}(\lambda_k) > 0$, which is fulfilled if and only if $\beta(\rho_k) < 0$, which is the standard condition for Turing instability in a spatially homogeneous system [18]. The solutions of (7) are evaluated for each k satisfying the above conditions to determine the largest value of λ_k .

The critical value of d and the critical value of ρ are obtained from the conditions $\beta(\rho_c) = 0$ and $d\beta(\rho_c)/d\rho_c = 0$, respectively, yielding

$$d_c = \frac{(J_{11}J_{22} - 2J_{12}J_{21}) - 2\sqrt{-J_{12}J_{21}\det(J)}}{J_{22}^2}, \quad (9)$$

and

$$\rho_c = \eta \frac{J_{11} + d_c J_{22}}{2d_c}. \quad (10)$$

It is worth mentioning that although (10) gives the theoretical maximizing space eigenvalue ρ_k , this maximum may not be attained since the wavenumbers k form a discrete set. The true maximizer will be the ρ_k which makes the real part of λ_k , the solution of (7), maximal [18]. On the other hand, the scale parameter η plays an important role because the range of wavenumbers that satisfy the instability conditions depends on this parameter. Therefore η can be increased to ensure that allowable wavenumbers exist in the unstable range of k [2]. This is illustrated in the following example.

2.1 Example: the Legendre equation

As a particular example, consider the Schnakenberg reaction-diffusion system [23], which has been frequently used because of its simple structure. In dimensionless form, we consider the following one-dimensional system in the space domain $\Omega = [-1, 1]$:

$$\frac{\partial u}{\partial t} = d \frac{\partial}{\partial x} \left(\mathcal{D}(x) \frac{\partial u}{\partial x} \right) + \eta (a - u + u^2 v) \quad (11a)$$

$$\frac{\partial v}{\partial t} = \frac{\partial}{\partial x} \left(\mathcal{D}(x) \frac{\partial v}{\partial x} \right) + \eta (b - u^2 v) \quad (11b)$$

$$\mathcal{D}(x) \frac{\partial u}{\partial x} = 0, \quad \mathcal{D}(x) \frac{\partial v}{\partial x} = 0 \quad \text{at } x = -1, 1, \quad (11c)$$

where a and b are positive constants. The Schnakenberg model is the simplest known two-component chemical reaction system that allows a limit cycle solution. Such a model involves three reactions (one of which is autocatalytic) for two chemical products X and Y and two chemical sources A and B ; in (11), x , y , a , and b are the respective concentrations. It has been one of the most studied models because it is simple and well behaved, and it has been applied to different problems of pattern formation, including plant root hair initiation [24] and reaction-diffusion equation systems coupled with convective flow [25].

The spectral problem (4) is the Sturm-Liouville problem:

$$\begin{aligned} \frac{d}{dx} \left(\mathcal{D}(x) \frac{d\Phi}{dx} \right) &= -\rho\Phi, \quad \text{in } \Omega = [-1, 1] \\ \mathcal{D}(x) \frac{d\Phi}{dx} &= 0, \quad \text{at } x = -1, 1. \end{aligned} \quad (12)$$

Let us consider first the case of homogeneous diffusion $\mathcal{D}(x) = 1$. In this case, we have $\Phi_k = \cos(kx)$ and $\rho_k = k^2 = (n\pi)^2$. The system (11) has a single equilibrium state at $(u_0, v_0) = (a+b, b/(a+b)^2)$, and the critical values (9) and (10) become

$$d_c = \frac{(a+b)(a+3b) - 2\sqrt{2b(a+b)^3}}{(a+b)^4}, \quad (13)$$

and

$$k_c^2 = \frac{(a+b)^4 \eta}{\sqrt{2b(a+b)^3} - (a+b)^2}. \quad (14)$$

Now, if $\mathcal{D}(x) = 1 - x^2$ the eigenfunctions of the Sturm-Liouville problem (12) $\Phi_k = P_k(x)$ are the Legendre Polynomials of degree $k \in \mathbb{N}$, with eigenvalues $\rho_k = k(k+1)$. In this case d_c is also (13), and

$$k_c(k_c + 1) = \frac{(a+b)^4 \eta}{\sqrt{2b(a+b)^3} - (a+b)^2}. \quad (15)$$

We numerically solve (11) with $a = 0.289$ and $b = 1.49$, and with (13) we calculate d_c yielding $d_c = 0.02735$. For Legendre diffusion, k is an integer; therefore we choose $k_c = 3, 11, 19$ and from (15) the corresponding value of the scale parameter η is calculated. This yields $\eta = 1.11571$, $\eta = 12.2729$ and $\eta = 35.3311$. Note that for homogeneous diffusion, k_c is given by (14), for which we have $k_c = 3.4641$, $k_c = 11.4891$ and $k_c = 19.4936$, respectively. In Fig. 1, patterns obtained at $T = 1000$ seconds with Legendre diffusion are compared with those obtained with homogeneous diffusion for the values given above.

Note that for the first two values of η , no pattern with homogeneous diffusion is formed however, for Legendre, diffusion patterns with the expected spatial modes are produced. For $\eta = 35.3310$ both patterns are formed with the expected spatial mode and the changes in wavelength in the case of Legendre diffusion is also observed.

For two-dimensional problems, the Schnakenberg reaction-diffusion sys-

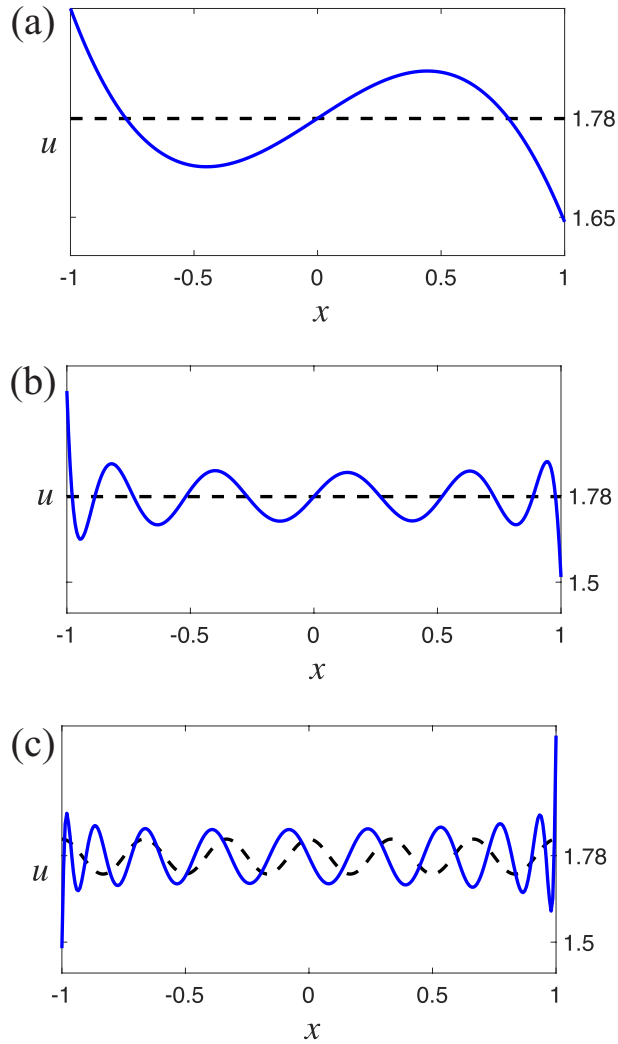


Figure 1: The patterns obtained at $T = 1000$ seconds with Legendre diffusion (blue continuous line) are compared to those obtained with homogeneous diffusion (black dashed line). **(a)** $\eta = 1.11571$, **(b)** $\eta = 12.2729$, and **(c)** $\eta = 35.3310$.

tem:

$$\frac{\partial u}{\partial t} = d \nabla \cdot (\mathcal{D}(\mathbf{x}) \nabla u) + \eta (a - u + u^2 v), \quad (16a)$$

$$\frac{\partial v}{\partial t} = \nabla \cdot (\mathcal{D}(\mathbf{x}) \nabla v) + \eta (b - u^2 v), \quad (16b)$$

is considered in the space domain $\Omega = [-1, 1] \times [-1, 1]$, and

$$\mathcal{D}(\mathbf{x}) \nabla u \cdot \mathbf{n} = 0, \quad \text{and} \quad \mathcal{D}(\mathbf{x}) \nabla v \cdot \mathbf{n} = 0, \quad (17)$$

on the boundaries of the square Ω .

For the spatial variation of the diffusion rate, $\mathcal{D}(x, y)$, we propose the following anisotropic tensor expression:

$$\mathcal{D}(x, y) = \begin{pmatrix} \begin{pmatrix} 1 - x^2 & 0 \\ 0 & 1 - y^2 \end{pmatrix} & 0 \\ 0 & \begin{pmatrix} 1 - x^2 & 0 \\ 0 & 1 - y^2 \end{pmatrix} \end{pmatrix}. \quad (18)$$

With this matrix, the spectral problem (4), in the space domain $\Omega = [-1, 1] \times [-1, 1]$, becomes

$$\frac{\partial}{\partial x} \left((1 - x^2) \frac{\partial \Phi_1}{\partial x} \right) + \frac{\partial}{\partial y} \left((1 - y^2) \frac{\partial \Phi_1}{\partial y} \right) = -\rho \Phi_1, \quad (19a)$$

$$\frac{\partial}{\partial x} \left((1 - x^2) \frac{\partial \Phi_2}{\partial x} \right) + \frac{\partial}{\partial y} \left((1 - y^2) \frac{\partial \Phi_2}{\partial y} \right) = -\rho \Phi_2. \quad (19b)$$

By separation of variables it can be shown that the eigenfunctions of this problem are

$$\Phi_m = \Phi_{ij}(x, y) = P_i(x)P_j(y), \quad (20)$$

where $m = 1, 2$, and eigenvalues

$$\rho = k_{ij} = i(i + 1) + j(j + 1). \quad (21)$$

The choice of (18) is forced by mathematical simplicity as any other choice could lead to a spectral problem that cannot be solved, as is the case with a simpler choice, such as $\mathcal{D}_{11} = \mathcal{D}_{22} = (1 - x^2)(1 - y^2)$. However, the form (18) is interesting in itself because, on the one hand, it produces a highly anisotropic diffusion, as described in Fig. 2, where an interpretation of the

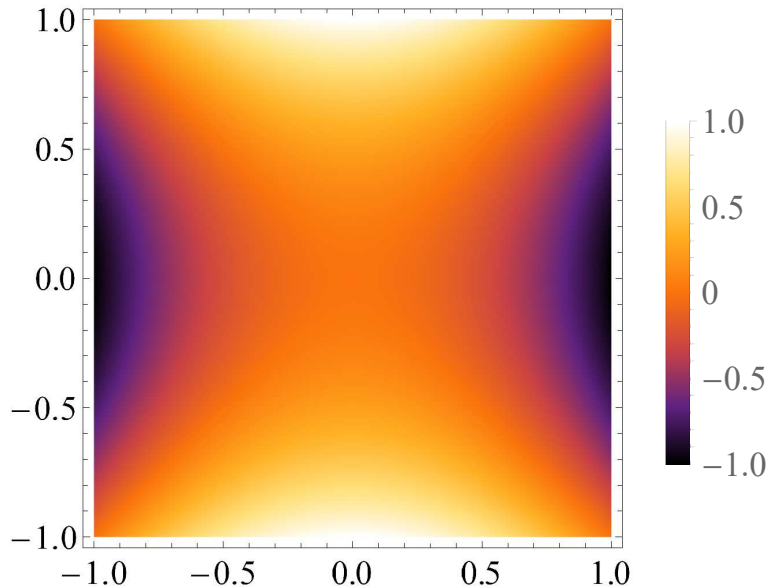


Figure 2: A graphical interpretation of the diffusion produced by (18); for each (x, y) , the difference in the diffusion coefficients, $(1 - x^2) - (1 - y^2)$, is plotted on a color scale. Positive values (light colors) indicate that concentrations move faster along the x -axis whereas negative values (dark colors) indicate that concentrations move faster along the y -axis.

spatial variation of the diffusion is given; for each (x, y) , the difference in the diffusion coefficients, $(1 - x^2) - (1 - y^2)$, is plotted on a color scale. Therefore, positive values (light colors) indicate that concentrations move faster along the x -axis whereas negative values (dark colors) indicate that concentrations move faster along the y axis. Thus, an initial concentration located near the central part of the right (or left) edge, moves faster along the y -axis than along the x -axis. In contrast, an initial concentration located near the central part of the top (or bottom) edge, moves faster along the x -axis. However, with (18), the operator in (19) is degenerate in the square $\Omega = [-1, 1] \times [-1, 1]$. For instance, the wave number $k_{i0} = k_{0i}$ in (21) has associate the eigenfunctions Φ_{i0} , Φ_{0i} , and the linear combination of both. This was required to generate striped and spotted patterns.

Because the linear analysis in the previous section is independent of the spatial dimension, the critical values d_c and k_c are given by (13) and (15), respectively. Some numerically obtained two-dimensional patterns will be

shown and explained in Sec. 4.

All numerical simulations in this study were carried out with the general-purpose finite element COMSOL Multiphysics[®] software [26], using Lagrange quadratic elements. A time step of $\Delta t = 0.001$ was used and the initial conditions were uniformly randomly generated around the steady state, with a range of 0.1. For one-dimensional problems, a highly refined mesh consisting of 100 evenly spaced space nodes was considered, and for two-dimensional problems, the refined mesh contained 24,912 domain elements and 400 boundary elements. Both spatial and time discretizations were tested by starting with larger values and verifying that further decrements did not modify the final form of the solution.

3 Nonlinear analysis for spatially varying diffusion: The Legendre eigenfunctions case

The spatially inhomogeneous solutions predicted by the linear analysis grow exponentially and then are not valid at all times. By means of a weakly nonlinear analysis, we can obtain approximate solutions that are valid for all the time. The standard nonlinear analysis developed for reaction-diffusion systems is based on the eigenfunctions of the Laplace operator, that is, $\mathcal{D}(\mathbf{x}) = 1$ in (4). To consider the Legendre operator (18), it is necessary to generalize this analysis based on the eigenfunctions $\Phi_{ij}(x, y) = P_i(x)P_j(y)$. Then the methodology developed in References [27, 28, 29] will be generalized for the orthogonal functions P_n , and the conditions for the generation of stripes and spots will be deduced. Before proceeding, we present some general results.

The Taylor series in two variables $\mathbf{u} = (u, v)$ around $\mathbf{u}_0 = (u_0, v_0)$, for the field $F = \eta(f, g)^T$, is given by:

$$F(\mathbf{u}) = F_0 + \eta J\mathbf{u} + Q(\mathbf{u}, \mathbf{u}) + C(\mathbf{u}, \mathbf{u}, \mathbf{u}) + \dots \quad (22)$$

Here $F_0 = \mathbf{0}$, and the linear term is the Jacobian matrix:

$$J = \begin{pmatrix} f_u & f_v \\ g_u & g_v \end{pmatrix}_{(u_0, v_0)}. \quad (23)$$

The general expressions for the quadratic and cubic terms, which will be required later, are

$$Q(\mathbf{u}_1, \mathbf{u}_2) = \frac{\eta}{2} \left(\begin{array}{c} f_{uu}u_1u_2 + f_{uv}u_1v_2 + f_{vu}v_1u_2 + f_{vv}v_1v_2 \\ g_{uu}u_1u_2 + g_{uv}u_1v_2 + g_{vu}v_1u_2 + g_{vv}v_1v_2 \end{array} \right)_{(u_0, v_0)}, \quad (24)$$

$$C(\mathbf{u}, \mathbf{u}, \mathbf{u}) = \frac{\eta}{6} \left(\begin{array}{c} f_u^3u_1^3 + 3f_{u^2v}u_1^2v_1 + 3f_{uv^2}u_1v_1^2 + f_v^3v_1^3 \\ g_u^3u_1^3 + 3g_{u^2v}u_1^2v_1 + 3g_{uv^2}u_1v_1^2 + g_v^3v_1^3 \end{array} \right)_{(u_0, v_0)}, \quad (25)$$

where $\mathbf{u} = (u, v)$, $\mathbf{u}_1 = (u_1, v_1)$, and $\mathbf{u}_2 = (u_2, v_2)$.

Finally, let $F_1 = (f_1, g_1)$ and $F_2 = (f_2, g_2)$ be two vector fields in a domain Ω . The inner product of F_1 and F_2 is defined by

$$\langle F_1 | F_2 \rangle = \langle (f_1, g_1) \cdot (f_2, g_2) \rangle = \int_{\Omega} (f_1f_2 + g_1g_2) d\mathbf{x}. \quad (26)$$

3.1 Multiscale method

Consider the following form of the reaction-diffusion system:

$$\frac{\partial \mathbf{u}}{\partial t} = D\nabla \cdot (\mathcal{D}(\mathbf{x})\nabla \mathbf{u}) + F(\mathbf{u}; p), \quad \text{in } \Omega \quad (27)$$

where $F(\mathbf{u}; p) = \eta(f(\mathbf{u}; p), g(\mathbf{u}; p))^T$, p is a parameter of the system, and η is a scale factor. The domain of the system is $\Omega = [-1, 1] \times [-1, 1]$, and Neumann (zero-flux) boundary conditions are considered:

$$\mathbf{n} \cdot (\mathcal{D}(\mathbf{x})\nabla \mathbf{u}) = 0, \quad \text{on } \partial\Omega. \quad (28)$$

The wavelength λ is perturbed around its bifurcation value λ_c as $\lambda = \lambda_c + \epsilon^2$, and close to the bifurcation point it is assumed that the solution of the equation is

$$\mathbf{u} = \mathbf{u}_0 + \hat{\mathbf{u}} = \mathbf{u}_0 + (\epsilon \mathbf{u}_1 + \epsilon^2 \mathbf{u}_2 + \epsilon^3 \mathbf{u}_3 + \dots). \quad (29)$$

The case $0 < \epsilon < 1$ is considered and a slow time scale is introduced:

$$T = \hat{w}t, \quad (30)$$

where

$$\hat{w} = \epsilon w_1 + \epsilon^2 w_2 + \dots. \quad (31)$$

A Taylor series expansion of F in (27), around the stable equilibrium point \mathbf{u}_0 , produces

$$F(\mathbf{u}) = \eta J \hat{\mathbf{u}} + Q(\hat{\mathbf{u}}, \hat{\mathbf{u}}) + C(\hat{\mathbf{u}}, \hat{\mathbf{u}}, \hat{\mathbf{u}}) + \dots, \quad (32)$$

where ηJ , Q and C are, respectively, the lineal quadratic and cubic terms.

By substituting (29) and (30) into (27), one obtains

$$\hat{w} \frac{\partial \hat{\mathbf{u}}}{\partial T} = D \nabla \cdot \mathcal{D}(\mathbf{x}) \nabla \hat{\mathbf{u}} + \eta J \hat{\mathbf{u}} + Q(\hat{\mathbf{u}}, \hat{\mathbf{u}}) + C(\hat{\mathbf{u}}, \hat{\mathbf{u}}, \hat{\mathbf{u}}) + \dots, \quad (33)$$

If additionally the parameter p of the model is perturbed about its value in a critical set:

$$p = p_c + \hat{p} = p_c + (\epsilon p_1 + \epsilon^2 p_2 + \dots),$$

then the expansion of (33) in a Taylor series around p_c , produces

$$\begin{aligned} \hat{w} \frac{\partial \hat{\mathbf{u}}}{\partial T} = & (D \nabla \cdot \mathcal{D}(\mathbf{x}) \nabla)^c \hat{\mathbf{u}} + \eta J^c \hat{\mathbf{u}} + Q^c(\hat{\mathbf{u}}, \hat{\mathbf{u}}) + C^c(\hat{\mathbf{u}}, \hat{\mathbf{u}}, \hat{\mathbf{u}}) + \dots + \\ & \hat{p}((D \nabla \cdot \mathcal{D}(\mathbf{x}) \nabla)_p^c \hat{\mathbf{u}} + \eta J_p^c \hat{\mathbf{u}} + Q_p^c(\hat{\mathbf{u}}, \hat{\mathbf{u}}) + \dots), \end{aligned} \quad (34)$$

where the subscripts stand for derivative with respect to p and the superscripts mean the evaluation at $p_c + \hat{p}$.

By proposing a solution of the form (29), this perturbation method produces a hierarchy of linear differential equations:

$$0(\epsilon) : \mathcal{L} \mathbf{u}_1 = \mathbf{0}, \quad (35)$$

$$0(\epsilon^2) : \mathcal{L} \mathbf{u}_2 = Q(\mathbf{u}_1, \mathbf{u}_1) + p_1 \eta J_p^c \mathbf{u}_1 - w_1 \frac{\partial \mathbf{u}_1}{\partial T}, \quad (36)$$

$$\begin{aligned} 0(\epsilon^3) : \mathcal{L} \mathbf{u}_3 = & Q(\mathbf{u}_1, \mathbf{u}_2) + C(\mathbf{u}_1, \mathbf{u}_1, \mathbf{u}_1) + p_2 \eta J_p^c \mathbf{u}_1 + p_1 \eta J_p^c \mathbf{u}_2 + \\ & p_1 \mathbf{Q}^c(\mathbf{u}_1, \mathbf{u}_1) - w_1 \frac{\partial \mathbf{u}_2}{\partial T} - w_2 \frac{\partial \mathbf{u}_1}{\partial T}, \end{aligned} \quad (37)$$

where $\mathcal{L} = (-\eta J - D \nabla \cdot \mathcal{D}(\mathbf{x}) \nabla)$. These equations will be solved in what follows.

$O(\epsilon)$ equations

In the presence of a Turing instability $\rho_{k_c} = k_{i_c 0} = k_{0 j_c}$ (see Eq. 21), and the solution of the linear problem can be written as the sum of N spatial modes. We consider the special case when two spatial modes are present ($N = 2$):

$$\mathbf{u}_1 = \mathbf{V}^{(1)} a(T) P_{i_c}(x) + \bar{\mathbf{V}}^{(1)} \bar{a}(T) P_{j_c}(y), \quad (38)$$

where P_k is the Legendre polynomial of degree k , and $k_{i_c j_c}$ satisfies the diffusion-driven instability conditions.

From (35) we have:

$$(-\eta J + k_{i_c j_c} D) \mathbf{V}^{(1)} = \mathbf{0}, \quad (39)$$

and the same for $\bar{\mathbf{V}}^{(1)}$. The solution of the above equation can be obtained and chosen to be a unitary vector, this is:

$$\mathbf{V}^{(1)} = \frac{1}{\sqrt{(-\eta g_v + d k_{i_c j_c})^2 + \eta^2 g_u^2}} \begin{pmatrix} -\eta g_v + d k_{i_c j_c} \\ \eta g_u \end{pmatrix}. \quad (40)$$

Since $i_c = j_c$, then $\mathbf{V}^{(1)} = \bar{\mathbf{V}}^{(1)}$.

In what follows, to simplify notation, we assume that $P_{i_c} = P_{i_c}(x)$, $\bar{P}_{j_c} = P_{j_c}(y)$, $a = a(T)$, and $\bar{a} = \bar{a}(T)$.

$O(\epsilon^2)$ equations

To solve the second equation, we begin by applying the Fredholm Alternative:

$$\left\langle \mathbf{u}^* \left| \mathbf{Q}(\mathbf{u}_1, \mathbf{u}_1) + p_1 \eta J_p^c \mathbf{u}_1 - w_1 \frac{\partial \mathbf{u}_1}{\partial T} \right. \right\rangle = 0, \quad (41)$$

where \mathbf{u}^* is in the null-space of the adjoint. Since the solution of the adjoint problem has the same form as the solution of the linear case, we propose

$$\mathbf{u}^* = \mathbf{V}^* a P_{i_c}, \quad (42)$$

or

$$\mathbf{u}^* = \bar{\mathbf{V}}^* \bar{a} \bar{P}_{j_c}. \quad (43)$$

The explicit form of $Q(\mathbf{u}_1, \mathbf{u}_1)$ can be obtained from (24) using (38). By doing this, we get:

$$\begin{aligned} \mathbf{Q}(\mathbf{u}_1, \mathbf{u}_1) = & Q(\mathbf{V}^{(1)}, \mathbf{V}^{(1)})a^2 P_{i_c}^2 + 2Q(\mathbf{V}^{(1)}, \bar{\mathbf{V}}^{(1)})\bar{a}a P_{i_c} \bar{P}_{j_c} + \\ & Q(\bar{\mathbf{V}}^{(1)}, \bar{\mathbf{V}}^{(1)})\bar{a}^2 \bar{P}_{j_c}^2. \end{aligned} \quad (44)$$

A key step is to expand the powers and products of P_{i_c} using the same basis functions, that is [30]:

$$P_q^2 = \sum_{n=0}^{2q} \xi_n P_n. \quad (45)$$

Consider first \mathbf{u}^* given by (42), then replacing (45) in (44), and the result in (41), together with (38), and applying the orthogonality properties of the eigenfunctions of the Legendre polynomials, we obtain

$$\xi_{i_c} \langle \mathbf{V}^* | Q(\mathbf{V}^{(1)}, \mathbf{V}^{(1)}) \rangle a^3 + p_1 \eta \langle \mathbf{V}^* | J_p^c \mathbf{V}_1 \rangle a^2 - w_1 \langle \mathbf{V}^* | \mathbf{V}_1 \rangle a \frac{\partial a}{\partial T} = 0. \quad (46)$$

In the case of odd Legendre polynomials, $\xi_{i_c} = 0$; hence, it is sufficient to guarantee that the perturbation parameter and time scale are canceled to ensure stable non-null patterns, that is, $p_1 = 0$ and $w_1 = 0$.

Once the Fredholm-Alternative is fulfilled, for the solution of the second order system, the following form is assumed:

$$\mathbf{u}_2 = \sum_{s=0}^{2i_c} (\mathbf{V}_s^{(2)} a^2 P_s + \bar{\mathbf{V}}_s^{(2)} \bar{a}^2 \bar{P}_s) + \mathbf{V}_{ij} a \bar{a} P_{i_c} \bar{P}_{j_c}, \quad (47)$$

where $\mathbf{V}_{ij} = \mathbf{V}_{ij}(x, y)$.

Substituting (47) and (38) into (36), and collecting the terms, we obtain the following coefficient vectors:

$$\mathbf{V}_s^{(2)} = (-\eta J + k_{s0} D)^{-1} \xi_s Q(\mathbf{V}^{(1)}, \mathbf{V}^{(1)}), \quad (48)$$

$$\bar{\mathbf{V}}_s^{(2)} = (-\eta J + k_{0s} D)^{-1} \xi_s Q(\bar{\mathbf{V}}^{(1)}, \bar{\mathbf{V}}^{(1)}), \quad (49)$$

$$\mathbf{V}_{ij} = 2(-\eta J + k_{ij} D)^{-1} Q(\mathbf{V}^{(1)}, \bar{\mathbf{V}}^{(1)}). \quad (50)$$

$O(\epsilon^3)$ equations

We again apply the Fredholm Alternative as follows:

$$\left\langle \mathbf{u}^* \left| Q(\mathbf{u}_1, \mathbf{u}_2) + C(\mathbf{u}_1, \mathbf{u}_1, \mathbf{u}_1) + p_2 \eta J_p^c \mathbf{u}_1 - w_2 \frac{\partial \mathbf{u}_1}{\partial T} \right. \right\rangle = 0. \quad (51)$$

By using (24) and (25), and (47) and (38), the quadratic and cubic terms of (51) can be obtained:

$$\begin{aligned} Q(\mathbf{u}_1, \mathbf{u}_2) = & \sum_{s=0}^{2i_c} (Q(\mathbf{V}^{(1)}, \mathbf{V}_s^{(2)}) a^3 P_{i_c} P_s + Q(\mathbf{V}^{(1)}, \bar{\mathbf{V}}_s^{(2)}) a \bar{a}^2 P_{i_c} \bar{P}_s + \\ & Q(\bar{\mathbf{V}}^{(1)}, \mathbf{V}_s^{(2)}) \bar{a} a^2 \bar{P}_{j_c} P_s + Q(\bar{\mathbf{V}}^{(1)}, \bar{\mathbf{V}}_s^{(2)}) \bar{a}^3 \bar{P}_{j_c} \bar{P}_s + \\ & Q(\mathbf{V}^{(1)}, \mathbf{V}_{ij}) a^2 \bar{a} P_{i_c}^2 \bar{P}_{j_c} + Q(\bar{\mathbf{V}}^{(1)}, \mathbf{V}_{ij}) a \bar{a}^2 P_{i_c} \bar{P}_{j_c}^2), \end{aligned} \quad (52)$$

and

$$\begin{aligned} C(\mathbf{u}_1, \mathbf{u}_1, \mathbf{u}_1) = & C(\mathbf{V}^{(1)}, \mathbf{V}^{(1)}) a^3 P_{i_c}^3 + 3C(\mathbf{V}^{(1)}, \bar{\mathbf{V}}^{(1)}) a^2 \bar{a} P_{i_c}^2 \bar{P}_{j_c} + \\ & 3C(\bar{\mathbf{V}}^{(1)}, \mathbf{V}^{(1)}) a \bar{a}^2 P_{i_c} \bar{P}_{j_c}^2 + C(\bar{\mathbf{V}}^{(1)}, \bar{\mathbf{V}}^{(1)}) \bar{a}^3 \bar{P}_{j_c}^3. \end{aligned} \quad (53)$$

Once again the product of the eigenfunctions can be represented as an expansion of the same eigenfunctions:

$$P_q P_{i_c} = \sum_n^{q+i_c} \zeta_n^{(q)} P_n, \quad P_{i_c}^3 = \sum_n^{3i_c} \chi_n P_n, \quad (54)$$

where the superscript (q) in the first expression indicates that the Fourier coefficient depends on the q -th eigenfunction.

Thus, substituting (54) and (45) in (52) and (53), we obtain

$$\begin{aligned} Q(\mathbf{u}_1, \mathbf{u}_2) = & \sum_{s=0}^{2i_c} \sum_{n=0}^{s+i_c} (Q(\mathbf{V}^{(1)}, \mathbf{V}_s^{(2)}) \zeta_n^{(s)} a^3 P_n + Q(\mathbf{V}^{(1)}, \bar{\mathbf{V}}_s^{(2)}) a \bar{a}^2 P_{i_c} \bar{P}_s + \\ & Q(\bar{\mathbf{V}}^{(1)}, \mathbf{V}_s^{(2)}) \bar{a} a^2 \bar{P}_{j_c} P_s + Q(\bar{\mathbf{V}}^{(1)}, \bar{\mathbf{V}}_s^{(2)}) \zeta_n^{(s)} \bar{a}^3 \bar{P}_n + \\ & Q(\mathbf{V}^{(1)}, \mathbf{V}_{ij}) \xi_s a^2 \bar{a} P_s \bar{P}_{j_c} + Q(\bar{\mathbf{V}}^{(1)}, \mathbf{V}_{ij}) \xi_s a \bar{a}^2 P_{i_c} \bar{P}_s), \end{aligned} \quad (55)$$

and

$$C(\mathbf{u}_1, \mathbf{u}_1, \mathbf{u}_1) = \sum_{n=0}^{3i_c} (C(\mathbf{V}^{(1)}, \mathbf{V}^{(1)})\chi_n a^3 P_n + 3C(\mathbf{V}^{(1)}, \bar{\mathbf{V}}^{(1)})\xi_n a^2 \bar{a} P_n \bar{P}_{j_c} + 3C(\bar{\mathbf{V}}^{(1)}, \mathbf{V}^{(1)})\xi_n a \bar{a}^2 P_{i_c} \bar{P}_n + C(\bar{\mathbf{V}}^{(1)}, \bar{\mathbf{V}}^{(1)})\chi_n \bar{a}^3 \bar{P}_n). \quad (56)$$

Now, (55), (56) and \mathbf{u}^* given by (42) are replaced into (51), and taking into account that $\zeta_i^{(q)} = 0$ for $q \leq i_c$ we get

$$\begin{aligned} \left\langle \mathbf{V}^* \left| \sum_{s=i_c+1}^{2i_c} Q(\mathbf{V}^{(1)}, \mathbf{V}_s^{(2)})\zeta_{i_c}^{(s)} \right. \right\rangle a^4 \delta_{i_0} + \left\langle \mathbf{V}^* \left| Q(\mathbf{V}^{(1)}, \bar{\mathbf{V}}_0^{(2)}) \right. \right\rangle a^2 \bar{a}^2 \delta_{i_0} + \\ \left\langle \mathbf{V}^* \left| Q(\bar{\mathbf{V}}^{(1)}, \mathbf{V}_{ij})\xi_0 \right. \right\rangle a^2 \bar{a}^2 \delta_{i_0} + \left\langle \mathbf{V}^* \left| C(\mathbf{V}^{(1)}, \mathbf{V}^{(1)})\chi_{i_c} \right. \right\rangle a^4 \delta_{i_0} + \\ \left\langle \mathbf{V}^* \left| 3C(\bar{\mathbf{V}}^{(1)}, \mathbf{V}^{(1)})\xi_0 \right. \right\rangle a^2 \bar{a}^2 \delta_{i_0} + \left\langle \mathbf{V}^* \left| p_2 \eta J_p^c \mathbf{V}^{(1)} \right. \right\rangle a^2 \delta_{i_0} - \\ \left\langle \mathbf{V}^* \left| \mathbf{V}^{(1)} \right. \right\rangle a \frac{da}{dT} \delta_{i_0} = 0, \quad (57) \end{aligned}$$

where $\delta_{i_0} = \int_{\Omega} (P_i \bar{P}_0)^2 dx dy$.

Equation 57 can be recasted as

$$\begin{aligned} \frac{1}{2} \left\langle \mathbf{V}^* \left| \mathbf{V}^{(1)} \right. \right\rangle \frac{d|a|^2}{dT} = \left\langle \mathbf{V}^* \left| \sum_{s=i_c+1}^{2i_c} Q(\mathbf{V}^{(1)}, \mathbf{V}_s^{(2)})\zeta_{i_c}^{(s)} + C(\mathbf{V}^{(1)}, \mathbf{V}^{(1)})\chi_{i_c} \right. \right\rangle a^4 + \\ \left\langle \mathbf{V}^* \left| Q(\bar{\mathbf{V}}^{(1)}, \mathbf{V}_{ij})\xi_0 + Q(\mathbf{V}^{(1)}, \bar{\mathbf{V}}_0^{(2)}) + 3C(\bar{\mathbf{V}}^{(1)}, \mathbf{V}^{(1)})\xi_0 \right. \right\rangle_w a^2 \bar{a}^2 + \\ \left\langle \mathbf{V}^* \left| p_2 \eta J_p^c \mathbf{V}^{(1)} \right. \right\rangle a^2. \quad (58) \end{aligned}$$

Finally, by repeating the same procedure, but for the second null vector (43), the Stuart-Landau amplitude equations are obtained:

$$\begin{aligned} \frac{d|a|^2}{dT} &= \alpha |a|^4 + \beta |a|^2 |\bar{a}|^2 + \theta |a|^2, \\ \frac{d|\bar{a}|^2}{dT} &= \alpha |\bar{a}|^4 + \beta |a|^2 |\bar{a}|^2 + \theta |\bar{a}|^2, \quad (59) \end{aligned}$$

where

$$E = \frac{1}{2} \langle \mathbf{V}^* | \mathbf{V}^{(1)} \rangle,$$

$$\alpha = \frac{1}{E} \left\langle \mathbf{V}^* \left| \sum_{s=i_c+1}^{2i_c} Q(\mathbf{V}^{(1)}, \mathbf{V}_s^{(2)}) \zeta_{i_c}^{(s)} + (\mathbf{V}^{(1)}, \mathbf{V}^{(1)}) \chi_{i_c} \right. \right\rangle, \quad (60)$$

$$\beta = \frac{1}{E} \left\langle \mathbf{V}^* \left| Q(\bar{\mathbf{V}}^{(1)}, \mathbf{V}_{ij}) \xi_0 + Q(\mathbf{V}^{(1)}, \bar{\mathbf{V}}_0^{(2)}) + 3C(\bar{\mathbf{V}}^{(1)}, \mathbf{V}^{(1)}) \xi_0 \right. \right\rangle, \quad (61)$$

$$\theta = \frac{1}{E} \left\langle \mathbf{V}^* \left| p_2 \eta J_p^c \mathbf{V}^{(1)} \right. \right\rangle. \quad (62)$$

3.2 Stability of the Stuart-Landau equations

The system (59) has 4 equilibrium points:

$$1) \quad |a|^2 = 0, \quad |\bar{a}|^2 = 0 \quad (63)$$

$$2) \quad |a|^2 = 0, \quad |\bar{a}|^2 = -\frac{\theta}{\alpha} \quad (64)$$

$$3) \quad |a|^2 = -\frac{\theta}{\alpha}, \quad |\bar{a}|^2 = 0 \quad (65)$$

$$4) \quad |a|^2 = -\frac{\theta}{\alpha + \beta}, \quad |\bar{a}|^2 = -\frac{\theta}{\alpha + \beta} \quad (66)$$

We are interested in the parameter regions where the equilibrium points are stable so that the Turing patterns are maintained for a long time. Using the corresponding Jacobian matrices, the conditions for the stability of each equilibrium point can be established to obtain the results summarized in Table 1.

Table 1: Steady states and conditions for linear stabilities of the amplitude functions.

Steady state	Conditions for linear stability	spatial pattern
$ a ^2 = \bar{a} ^2 = 0$	$\theta < 0$	None
$ a ^2 = 0, \bar{a} ^2 = \frac{-\theta}{\alpha}$	$\theta > 0$ and $\frac{\beta}{\alpha} > 1$	Stripes
$ a ^2 = \frac{-\theta}{\alpha}, \bar{a} ^2 = 0$	$\theta > 0$ and $\frac{\beta}{\alpha} > 1$	Stripes
$ a ^2 = \bar{a} ^2 = \frac{\theta}{\alpha + \beta}$	$\theta > 0$ and $\alpha < - \beta < 0$	Spots

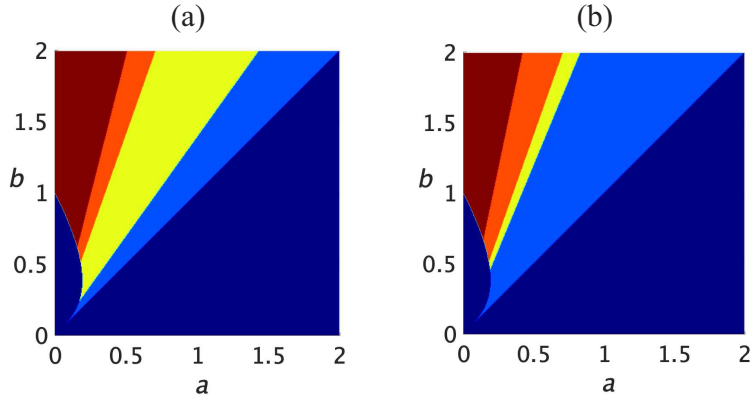


Figure 3: Parameter space (a, b) of the Schnakenberg model with homogeneous diffusion (a) and Legendre diffusion (b). Red color represents stripes, orange color represents spots, yellow color represents patterns that cannot be predicted by the nonlinear analysis, and blue light and dark colors represent the region where the stability and instability Turing conditions are not fulfilled, respectively.

4 Numerical simulations

Here we consider the two-dimensional Schnakenberg system (16) with zero-flux boundary conditions (17). For this system, the results of the non linear analysis, summarized in Table 1 can be used to divide the parameter space (a, b) into domains corresponding to different spatial patterns. For comparison purposes, homogeneous diffusion, $\mathcal{D}(x) = 1$, and Legendre diffusion, where $\mathcal{D}(\mathbf{x})$ is given by (18), are considered.

The results are shown in Fig. 3, where the regions where spatial patterns are stripes, spots, when the non linear analysis cannot predict a particular pattern and when the conditions for a Turing instability are not satisfied are indicated with colored regions. Red color represents stripes, orange color represents spots, yellow color represents patterns that cannot be predicted by the non linear analysis, and blue light and dark colors represent the region where the stability and instability Turing conditions are not fulfilled, respectively. Fig. 3a corresponds to the case of homogeneous diffusion, where a spatial mode $k_c = 4\pi$, that is, $n = 4$, was chosen. Fig. 3b corresponds to the case of Legendre diffusion with spatial modes $k_c = 3$, which corresponds to $k_{30} = k_{03} = 12$ in (21). The procedure for generating the plots is as follows.

For each of the two cases, with the established value of k_c , for a given mapped point (a, b) , a suitable value of η is calculated using (14) and d_c is calculated using (13). With these values, the parameters α , β and θ were evaluated, and the conditions listed in the second column of Table 1 were used to determine the type of pattern that was generated. The regions in red are for patterns that cannot be predicted by the present nonlinear analysis, which means that for (a, b) in these regions none of the four conditions for linear stability of the Stuart-Landau equations, in the second column of Table 1, is satisfied. However, because for these values of (a, b) the conditions for Turing instability are fulfilled, a pattern is formed. This pattern is typically observed with an irregular distribution of spots.

It is observed that the region of patterns that cannot be predicted by the linear analysis is reduced in the case of Legendre diffusion as compared with homogeneous diffusion. By contrast, the region where the Turing stability condition is not fulfilled is enlarged.

The two-dimensional Schnakenberg system is solved to numerically verify the predictions for Legendre diffusion in Fig. 3b for some values of parameters a and b . Regarding homogeneous diffusion, Fig. 3a was already obtained for the Schnakenberg system in [29] (Fig. 8b in that work), and the plots match.

Because the nonlinear analysis is performed at critical values, once a pair (a, b) is selected, d is chosen to satisfy (13) and η is obtained from (14) or (15) to satisfy a given k_c . To generate an initial growth of the spatial pattern, parameters a and b were perturbed by $\Delta a = 0.001$ and $\Delta b = 0.01$.

Three sets of parameters (a, b) were chosen in different regions of Fig. 3b, and they are given in Table 2. Two cases were considered, $k_c = 3$ (as in Fig. 3b) and $k_c = 14$.

The resulting patterns are shown in Fig. 4. We observed that the predictions of the nonlinear analysis were numerically validated. In addition, the spatial variation in the diffusion rate, in accordance with Fig. 2, is clearly observed in the figures on the right.

5 Discussion

A problem of pattern formation with reaction-diffusion equations with space varying diffusion is discussed. This problem corresponds to diffusion coefficients with explicit dependence on spatial variables. The first part of the

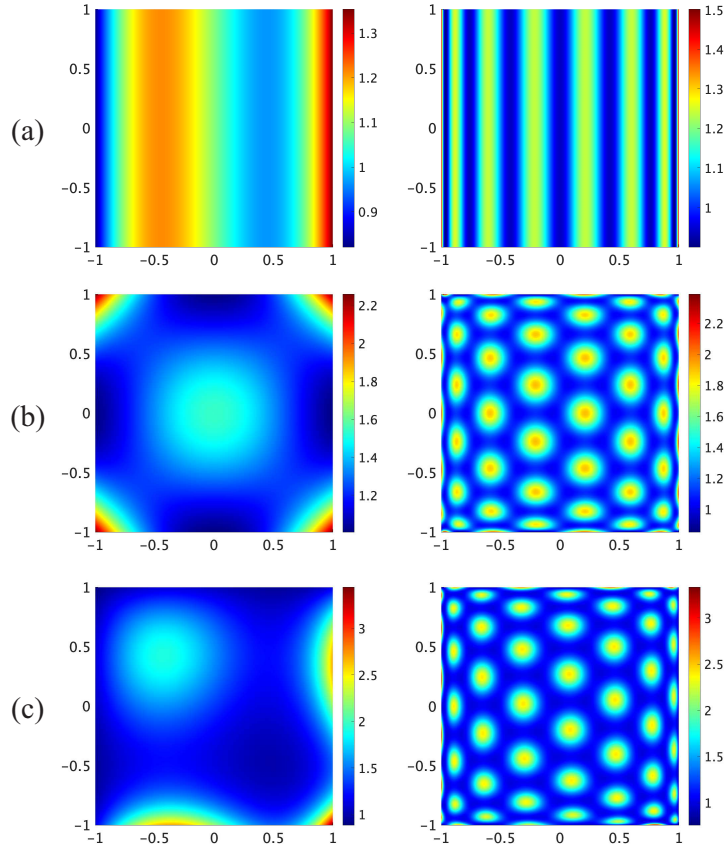


Figure 4: Two-dimensional patterns obtained numerically for three sets of parameters (a, b) , and two values of k_c . The left plots correspond to $k_c = 3$ and the right plots correspond to $k_c = 14$. The three rows correspond to different values of (a, b) : **(a)** $(0.1, 1.0)$ in the region of stripes, **(b)** $(0.3, 1.0)$ in the region of spots, and **(c)** $(0.375, 1.0)$ in the region where our linear analysis cannot predict the type of pattern; in all cases u is plotted. The parameter values are presented in Table 2.

mathematical analysis of this problem, the linear analysis, can be performed for general space-dependent diffusion coefficients [18], and the main results are reviewed in Sec. 2. The second part however, requires a generalization of the standard weakly nonlinear analysis for eigenfunctions other than the eigenfunctions of the Laplace operator. In this study, we consider the particular case of the operator $\partial_x((1-x^2)\partial_x)$, whose eigenfunctions are the Leg-

Table 2: The model parameters of the Schnakenberg system (16) used in Fig. 4. (a, b) were chosen at different regions in Fig. 3b. For each (a, b) , d_c was calculated using (13). Two values of k_c are used: $k_c = 3$ and $k_c = 14$. The corresponding values of η were obtained using (15).

(a, b)	Region	d_c	k_c	η
(0.1, 1.0)	Stripes	0.1003	3	3.4552
			14	60.466
(0.3, 1.0)	Spots	0.0342	3	1.7066
			14	29.866
(0.375, 1.0)	Not predicted	0.0224	3	1.3078
			14	22.866

endre polynomials $P_n(x)$, and eigenvalues $n(n+1)$. For the two-dimensional problem we propose a tensor form for the spatial variation of the diffusion rate, which leads to a Sturm-Liouville problem with eigenfunctions given by $P_{ij}(x, y) = P_i(x)P_j(y)$ and eigenvalues $i(i+1) + j(j+1)$. With these functions, a generalization of the weakly nonlinear analysis is proposed. This generalization allows us to find conditions for the formation of stripped or spotted patterns, which are verified numerically, and compared with the case of homogeneous diffusion, using the Schnakenberg reaction-diffusion system as an example .

Some differences arise with the standard non linear analysis, of which it is worth highlighting the appearance of Fourier coefficients ξ_n , $\zeta_n^{(q)}$, and χ_n , which vary with the critical wave number, contrary to the case of the eigenfunctions of the Laplace operator where they remain constant. This can produce variations in terms of the amplitude equations and asymmetries when the critical wavenumber is modified, which is worth exploring further.

It must be said that it is tempting to attempt a generalization of nonlinear analysis for orthogonal eigenfunctions of any Sturm-Liouville problem, where the Legendre functions are a particular case. This general approach faces several difficulties, mainly with the Fredholm alternative, which we are currently working on.

The type of patterns generated by the particular problem studied in this work enriches the field of pattern formation and the generalization of the nonlinear analysis developed here can also be of interest in other fields such as climate modeling [21, 22] and can motivate further generalization by using

orthogonal eigenfunctions of any Sturm-Liouville problem.

Acknowledgments

This work was supported by CONACYT under Project No. A1-S-8317. Elkin A. Calderón-Barreto received Fellowship 995896 from CONACYT.

References

- [1] A. M. Turing, The chemical basis of morphogenesis, *Philos Trans R Soc Lond Ser B Biol Sci* 237 (1952) 37–72.
- [2] J. D. Murray, *Mathematical Biology vol. II. Spatial Models and Biomedical Applications*, 3rd Edition, Springer, New York, 2003.
- [3] S. Kondo, T. Miura, Reaction-diffusion model as a framework for understanding biological pattern formation, *Science* 329 (5999) (2010) 1616–1620.
- [4] A. L. Krause, E. A. Gaffney, P. K. Maini, V. Klika, Modern perspectives on near-equilibrium analysis of turing systems, *Phil. Trans. R. Soc. A* 379 (2213) (2021) 20200268.
- [5] P. K. Maini, D. L. Benson, J. A. Sherratt, Pattern formation in reaction-diffusion models with spatially inhomogeneous diffusion coefficients, *IMA J. Math. Appl. Med. Biol.* 9 (1992) 197–213.
- [6] D. L. Benson, P. K. Maini, J. A. Sherratt, Unravelling the turing bifurcation using spatially varying diffusion coefficients, *J. Math. Biol.* 37 (1998) 381–417.
- [7] J. Wei, M. Winter, Spikes for the gierer-meinhardt system with discontinuous diffusion coefficients, *J. Nonlinear Sci.* 19 (2009) 301–339.
- [8] J. A. Sherratt, Turing bifurcations with a temporally varying diffusion coefficient, *J. Math. Biol.* 33 (1995) 295–308.
- [9] M. R. Roussel, J. Wang, Pattern formation in excitable media with concentration-dependent diffusivities, *J. Chem. Phys.* 120 (2004) 8079–8088.

- [10] G. Gambino, M. Lombardo, M. Sammartino, V. Sciacca, Turing pattern formation in the brusselator system with nonlinear diffusion, *Phys. Rev. E* 88 (2013) 042925.
- [11] D. Das, Turing pattern formation in anisotropic medium, *J. Math. Chem.* 55 (3) (2017) 818–831.
- [12] K. Page, P. K. Maini, N. A. Monk, Pattern formation in spatially heterogeneous turing reaction-diffusion models, *Physica D: Nonlinear Phenomena* 181 (2003) 80–101.
- [13] K. M. Page, P. K. Maini, N. A. Monk, Complex pattern formation in reaction–diffusion systems with spatially varying parameters, *Physica D: Nonlinear Phenomena* 202 (1-2) (2005) 95–115.
- [14] G. Chacón-Acosta, M. Núñez López, I. Pineda, Turing instability conditions in confined systems with an effective position-dependent diffusion coefficient, *J. Chem. Phys.* 152 (2020) 024101.
- [15] B. Liu, R. Wu, N. Iqbal, Turing patterns in the lengyel–epstein system with superdiffusion, *Int. J. Bif. Chaos* 27 (8) (2017) 1730026.
- [16] D. Hernández, E. C. Herrera-Hernández, M. Núñez López, H. Hernández-Coronado, Self-similar turing patterns: An anomalous diffusion consequence, *Phys. Rev. E* 95 (2017) 022210.
- [17] H. K. Khudhair, Y. Zhang, N. Fukawa, Pattern selection in the schnakenberg equations: From normal to anomalous diffusion, *Numer. Methods Partial Differ. Eq.* 38 (6) (2022) 1843–1860.
- [18] R. A. Van Gorder, Pattern formation from spatially heterogeneous reaction-diffusion systems, *Phil. Trans. R. Soc. A* 379 (2213) (2021) 20210001.
- [19] R. Dillon, P. Maini, O. H.G., Pattern formation in generalized turing systems i. steady-state patterns in systems with mixed boundary conditions, *J. Math. Biol.* 32 (1994) 345—393.
- [20] M. Kozák, G. A. Eamonn, V. Klika, Pattern formation in reaction-diffusion systems with piecewise kinetic modulation: An example study of heterogeneous kinetics, *Phys. Rev. E* 100 (4) (2019) 042220.

- [21] G. R. North, Theory of energy-balance climate models, *J. Atmos. Sci.* 32 (11) (1975) 2033–2043.
- [22] G. Hetzer, The number of stationary solutions for a one-dimensional budyko-type climate model, *Nonlinear Anal. RWA* 2 (2001) 259–272.
- [23] J. Schnakenberg, Simple chemical reaction systems with limit cycle behaviour, *J. Theor. Biol.* 81 (3) (1979) 389–400.
- [24] V. Breña Medina, A. R. Champneys, C. Grierson, M. J. Ward, Mathematical modeling of plant root hair initiation: Dynamics of localized patches, *SIAM J. Appl. Dyn. Syst.* 13 (1) (2014) 210–248.
- [25] J. Wei, M. Winter, Flow-distributed spikes for schnakenberg kinetics, *J. Math. Biol.* 64 (2012) 211–254.
- [26] COMSOL AB, Stockholm, Comsol multiphysics® v.6.0., www.comsol.com (2022).
- [27] B. Ermentrout, Stripes or spots? nonlinear effects in bifurcation of reaction-diffusion equations on the square, *Proc. R. Soc. Lond. A* 434 (1991) 413–417.
- [28] T. Mahar, B. Matkowsky, A model biochemical reaction exhibiting secondary bifurcation, *SIAM Journal on Applied Mathematics* 32 (2) (1977) 394–404.
- [29] M. Zhu, J. Murray, Parameter domains for generating spatial pattern: a comparison of reaction–diffusion and cell-chemotaxis models, *International Journal of Bifurcation and Chaos* 5 (06) (1995) 1503–1524.
- [30] J. Dougall, The product of two legendre polynomials, *Proc. Glasg. Math. Assn.* 1 (3) (1953) 121–125.